Modeling of the Urothelium with an Agent Based Approach

Angelo Torelli[1], Fabian Siegel[2], Philipp Erben[2], and Markus Gumbel[1,⋆]

[1] Institute for Medical Informatics, Mannheim University of Applied Sciences
{a.torelli,m.gumbel}@hs-mannheim.de
http://www.hs-mannheim.de
[2] Clinic of Urology, Medical Faculty Mannheim at the University of Heidelberg
{fabian.siegel,philipp.erben}@medma.uni-heidelberg.de
http://www.umm.de

Abstract. Novel models for cell differentiation and proliferation in the urothelium are presented. The models are simulated with the Glazier-Graner-Hogeweg technique using CompuCell3D. From a variety of tested models, the *contact model* is the best candidate to explain cell proliferation in the healthy urothelium. Based on this model, four variations were compared to highlight the key variations that best fit real urothelium. All simulations were quantified by a fitness function designed for the requirements of the urothelium. The findings suggest that adhesion and a nutrient dependent growth may play a crucial role in the maintenance of the urothelium. Aberrations in either adhesion or nutrient dependent growth led to the development of polyp-like formations. This work mimics the regeneration process and the steady state of the urothelium with a spatial and adhesion dependent approach for the first time.

Keywords: Agent-based, Glazier-Graner-Hogeweg, Monte Carlo, Simulation, Urothelium.

1 Introduction

Bladder cancer is the sixth most common cancer in men [1]. Although cancer can spread from neighboring organs to invade and grow in the bladder, the most common form of bladder cancer originates within the bladder's epithelial wall, the urothelium (see figure 7c). The urothelium is the tissue separating the intraluminal space, which in this case is filled with urine, and the interstitial fluid and is made of different layers, starting from a single layer of basal cells (in the sequel denoted as B and colored orange) and stem cells (S, blue) laying on top of the basal membrane (BM, red). These cell types are followed by three to five layers of intermediate cells (I, green). The urothelium ends at the bladder lumen with a single layer of specialized umbrella cells (U, gray), protecting its progenitors underneath [2]. This stratified epithelium of the bladder is anchored down on the lamina propria through the basal membrane, which is more a matrix than a

⋆ Corresponding author.

F. Ortuño and I. Rojas (Eds.): IWBBIO 2015, Part II, LNCS 9044, pp. 375–385, 2015.

membrane and is made up mostly of type-IV collagen, microfibrils and laminin [3]. The basal membrane also acts as a mechanical barrier, preventing malignant cells from invading the deeper tissues [4] and it is essential for angiogenesis [5].

Surprisingly, many characteristics of each bladder cell type are still unknown. For instance various hypotheses of cell lineages (The description of the history of the types of the cell progeny) of the urothelium have been postulated [6, 7, 8], but none has yet been proven. Only a few models *in silico* of the urothelium have been published, such as [9] in which the matrix metalloproteinase in the urothelium was analyzed by means of a cellular automaton.

In the course of the literature search, no previous work was found that simulates the urothelium in a healthy state for the purpose of better understanding of its architecture, lineage and function. Therefore, we extended the cellular automata approach. The aim for this work was: 1) to simulate the urothelium in both its normal healthy steady state, as well as 2) to test the stability of the tissue in a damaged or stressed state with the Glazier-Graner-Hogeweg (GGH) technique [10]. The GGH approch is a lattice-based Monte-Carlo simulation method that minimizes an energy function. Objects of the simulation are described and influenced by this energy function. We utilized the CompuCell3D framework [11], which is based on the GGH-model. Because of the lack of understanding of the function of each individual cell, various elementary models were set up parallel to each other to compare the biological facts with the hypotheses made in this work. The focus of our work is on tissue simulation and cell arrangements. Molecular aspects and physical forces, such as the expansion and contraction of the bladder, were not included yet.

This paper is organized in the following way: section *methods* explains the approach of developing models that in turn will compete against each other to be the model to best fit real anatomical tissue. This comparison will be based on a fitness value developed during this work and will also be explained in detail. Section *results* displays the benchmark of each of the models that will be discussed in the following sections *discussion* and *conclusion*.

2 Methods

The simulated models were run for an equivalent period of up to 2 years. All simulations start with two stem cells attached on the basal membrane. After about three to ten days, the urothelium should be regenerated and reaches a steady state [12]. 1440 Monte-Carlo-Steps (MCS) according to the GGH approach represents a day. The GGH-lattice has the dimensions $x \cdot y \cdot z$ equivalent to $150 \cdot 200 \cdot 1$ representing the total observed volume $V_{max} = 150 \cdot 200 \cdot 1 = 3 \cdot 10^4 \mu m^3$ for all simulations, with one voxel having the volume $1\mu m$. The shape of a cell can be controlled in GGH-models by surface- and volume-constraint-parameters. These parameters were set in all models such that cells keep their target volume with little variation, but have a flexible surface. Thus, cells are deformable.

2.1 Biological Processes

Each of the developed representations of the urothelium consist of different components, which can be categorized into four biological processes: 1) birth, 2) death, 3) differentiation, and 4) sorting. These can then be combined – along with their parameter set – to create new, sophisticated models.

Birth- and Death Process. The diffusion of nutrients in the urothelium has been included. The growth of the cell can either be infinite (abbreviated as IN) or nutrient dependent (NU). An infinite growth lets all cells proliferate according to its cell lineage (see Differentiation Process). In contrast, nutrient dependent growth lets cells only proliferate if a minimum of nutrients is available. Nutrients diffuse from the lamina propria through the basal membrane and are consumed by the adjacent cells. We have set the diffusion parameters such that nutrients reach into half of the urothelium. When cells grow and have reached their maximum (target) size they undergo mitosis. This implies a cell cycle period.

A cell can die, either through apoptosis, or mechanically through the process of voiding. Apoptosis is, in our simulations, set differently for each cell type to about 90, 30 and 10 days accordingly for the basal, intermediate and umbrella cells. Voiding of the bladder occurs every six hours. Here, apical cells that are in contact with the bladder lumen are randomly removed (washed out) with a probability of 2%. The stem cell does not undergo apoptosis, but can be washed away if it reaches the surface.

Differentiation Process. Figures 1, 2 and 3 show possible cell division scenarios for each cell type. A cell can either divide, which is expressed by a plain line, or transform (differentiate), which is expressed by a dashed line. Division can occur either symmetrically (fig. 1a, 1b, 2a, 2b and 3a) or asymmetrically (fig. 1c and 2c). Tranformation happens either through contact (fig. 2e and 3c) or through time (fig. 2d). The special case of fusion has been included (fig. 3b), which is when more than one intermediate cell becomes an umbrella cell. This phenomenon is discussed in [13, 14]. All these approaches can form various cell lineages when they are combined. Different models were derived from these combinations and have been tested, but only four were compared (cf. section 3).

Sort Process. As tissue formation is far from being random, we assume a sorting process. The tissue can sort itself either randomly (RA) or based on the differential adhesion hypothesis [15, 16]. In case of a random sort process, all cells have the same adhesion value of 1 independently of their cell type. When differential adhesion is applied, cells have a specific adhesion according to their cell types and contact to one another and other cell types. Table 1 shows the adhesion energies used. The energies were assigned according to values taken from the literature for two cell types (e. g. [16]) and adjusted for four cell types and its environment. The split axis is vertical and parallel to the basal membrane.

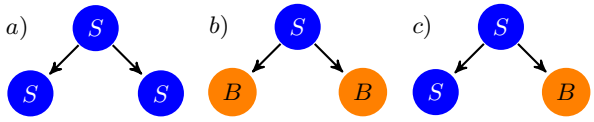

Fig. 1. Possible cell divisions for stem cells. S: Stem cell, B: Basal cell

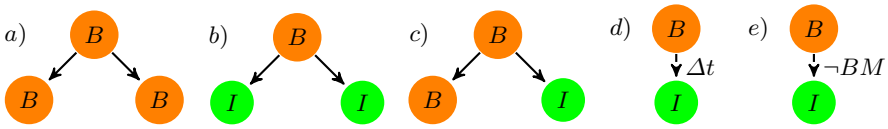

Fig. 2. Possible cell divisions for basal cells. B: Basal cell, I: Intermediate cell, BM: Basal membrane, Δt = cell cycle time.

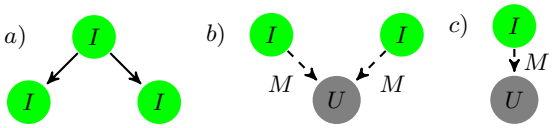

Fig. 3. Possible cell divisions for intermediate cells. I: Intermediate cell, U: Umbrella cell, M: Medium (urine)

Table 1. Differential adhesion energies used in all DAE-simulations. A small value represents stickiness, greater values less adhesion. M: Medium (urine), BM: basal membrane, S: stem cell, B: basal cell, I: intermediate cell, U: umbrella cell. Note that the matrix is symmetrical.

Types	M	BM	S	B	I	U
M	0	14	14	14	14	4
BM		0	1	3	12	12
S			6	4	8	14
B				5	8	12
I					6	4
U						2

2.2 Fitness Function

Finally, we have introduced a method for measuring the fitness of the model. This model is based on the arrangement and the volume of the simulated tissue compared with the observed biological data.

The fitness functions (see eq. 1) consist of a weighted fitness function for: 1) the arrangement of cells and 2) the volume of the cells. The fitness is measured at specific points in time t_i, typically starting from $t_1 = 20$ d (days) to the end of the simulation. All functions in this paper are dependent on time, such as $f(t_i)$, but for the sake of simplicity it will be referred to as f. Both functions are described in detail later in this section.

$$f = \frac{\bar{f}_a + f_v}{2} \,. \tag{1}$$

Thus, f enables us to quantify the results and to process the simulations in batch-mode, which serves as an input for parameter optimization. The fitness values were recorded throughout the entire simulation with a rate of a simulated half-day equaling 720 MCS, making one MCS equivalent to one minute.

Arrangement Fitness Function. The arrangement fitness function f_a surveys models to ensure that the cell strata are in the correct order. To ensure the correct order of the tissue, columnar samples are taken throughout the entire width of the tissue with steps of $20\mu m$. The columnar samples are vertical extractions of the tissue where fragments of little squares of two by two voxels are taken every $7\mu m$. Each of these voxels can be occupied by only one cell. To avoid duplicates, the most frequently occurring cell will be taken into account and inserted into a stack only once. This stack then undergoes further analysis done by a function applying Boolean terms. This analysis reaches an optimum of 1 if the urothelium reaches a state where the basal and stem cells layer is right above the basal membrane, followed by the various layers of intermediate cells and finally with one layer of umbrella cells before the lumen, and finally, the medium (urine), occupying the intraluminal space. In the worst case scenario, 0, the simulation does not create any cells at all. The arrangement fitness function is summarized in equation 2:

$$f_a = \begin{cases} \frac{1}{(1-L_B)+(L-L_I)+(1-L_U)+1} & \text{if } L_B + L + L_U > 0 \\ 0 & \text{otherwise .} \end{cases} \tag{2}$$

Where $(1 - L_B) + (L - L_I) + (1 - L_U)$ represents the number of cells that wandered away from their intended layer, described as followed:

- $L_B = 1$ if the first layer is made of cell type basal or stem, otherwise 0.
- $L_U = 1$ if the last layer is made of cell type umbrella, otherwise 0.
- L is the number of strata in between the first and last layer, while L_I is the subset of L counting the layers made of intermediate cells.

The function f_a is then calculated column by column on $n = 7$ different locations within the tissue. Out of these values, the average is taken as follows:

$$\bar{f_a} = \frac{1}{n} \sum_{i=1}^{n} f_a(i) \ . \tag{3}$$

Volume Fitness Functions. Since no information was found in the literature search regarding the volume of each of the urothelial cell types, values for the tissue height and for volume occupied by each cell type in percentage were calculated as an average from a variety of histological pictures of the urothelium that were found in these sources [17, 18, 19, 20, 21]. The average height of the urothelium is estimated to be $85\mu m$, which helps to determine the optimal volume a simulated urothelium should reach V_{opt} and is equal to

$150\mu m \cdot 85\mu m \cdot 1\mu m = 1.275 \cdot 10^4 \mu m^3$. Furthermore, umbrella cells were estimated to occupy 23%, intermediate cells occupy 67% and basal and stem cells together occupy 10% of the entire tissue volume respectively. With these values, it is possible to have an idea if the simulation is accurately representing the urothelium or not, by using S_B, S_I and S_U as the ideal volumes of each cell types. This is done by using a fitness function for each cell type f_B, f_I and f_U which are defined in equation 4.

$$f_B = \frac{1}{\frac{(S_B - I_B)^2}{a \cdot V_{max}} + 1}, \; f_I = \frac{1}{\frac{(S_I - I_I)^2}{a \cdot V_{max}} + 1}, \; f_U = \frac{1}{\frac{(S_U - I_U)^2}{a \cdot V_{max}} + 1} \; . \tag{4}$$

with

- $S_B = 10\% \cdot V_{opt}$, $S_I = 67\% \cdot V_{opt}$ and $S_U = 23\% \cdot V_{opt}$ are the ideal volumes of each cell types.
- I_B, I_I and I_U are the actual volumes of each cell type.
- $V_{max} = 3 \cdot 10^4 \mu m^3$ is the maximum volume all cell types can occupy.
- $a = 3\mu m^3$ is a factor that regulates the width of each volume fitness function.

The fitness functions f_B, f_I and f_U could be treated individually as shown in figure 4, but are merged together into one volume fitness function f_v that describes the entire volume of the tissue as shown in equation 5.

$$f_v = \begin{cases} (f_B + f_I + f_U)/3 & \text{if } 0 < I_B,\ I_I \text{ or } I_U < V_{max} \\ 0 & \text{otherwise .} \end{cases} \tag{5}$$

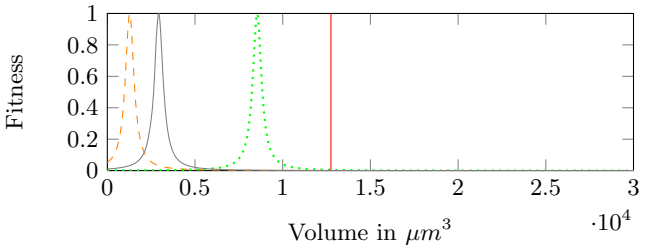

Fig. 4. Volume functions f_B (orange, dashed) with peak at 10% of V_{opt}, f_U (solid, gray) with peak at 23% of V_{opt}, and f_I (green, dotted) with peak at 67% of V_{opt} and V_{opt} as a vertical line (red). The x-axis extends from 0 to V_{max}.

3 Results

Among the various hypotheses we have tested, the so called *contact model* was very successful (cf. 5) based on the fitness function. Therefore, the *contact model* was further analyzed with four variations. We have also simulated many more models that can be derived from the differentiation process as shown in

figures 1, 2 and 3. Their fitness was very poor and were consequently rejected for candidates for the healthy urothelium (data not shown).

The contact model states that stem cells living in the basal layer above the basal membrane are the main source of proliferation. From there, the different cell types are formed through transformation triggered by contact change, following a certain cell lineage hierarchy. It should be added that every model also includes the voiding and apoptosis process (described previously) and is therefore not marked as such separately. The variations of the contact model are the four combinations:

1. NU-RA: Nutrient-dependent growth and random sort process.
2. NU-DAE: Nutrient-dependent growth and differential adhesion sort process.
3. IN-RA: Infinite growth and random sort process.
4. IN-DAE: Infinite growth and differential adhesion sort process.

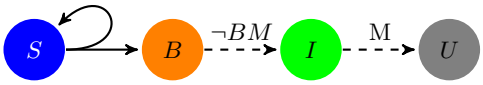

Fig. 5. Cell lineage of the contact model. S: Stem cell, B: Basal cell, BM: Basal membrane, I: Intermediate cell, M: Medium (urine), U: Umbrella cell

These are compared based on their fitness as shown in figure 6. Because the urothelium has a regeneration time between three and ten days, only fitness values after 20 days (or 28800 MCS) were taken into account. This ensures that all the simulations were in steady state. For each simulation run, the mean fitness of all points in time was calculated and these values were grouped by the model-variation and summarized as a box-and-whisker plot (see fig. 6).

Clearly, models with a random sort process, i. e. the same adhesion, do not form an urothelium-like tissue. We often observed simulations (IN-RA, NU-RA) where a stem cell had drifted to the surface of the urothelium and then washed out by the voiding process. With the disappearance of the cell source, the tissues disappear shortly after by an average of 60 days. However, the variance is remarkable. Figure 7a) shows an example of a simulation with no sort process, where only few basal cells are present and the protective umbrella cells engulf the urine and transport it inside the tissue jeopardizing the protective function of the urothelium.

On the other hand, contact models with a sort process based on differential adhesion show a significantly better behavior. On average over time, they reach a fitness of about 56% (IN-DAE) and 60% (NU-DAE). Nutrient-based growth leads to a striking smaller variance and extreme values for the overall fitness.

A representation of the NU-DAE-based urothelium *in silico* with a fitness of about 95% at 230 days is shown in figure 7b). The simulated tissue has a great similarity to the histological image of a healthy human urothelium, as depicted in figure 7c), in that it has the same number of layers and a corresponding order and size of cell types.

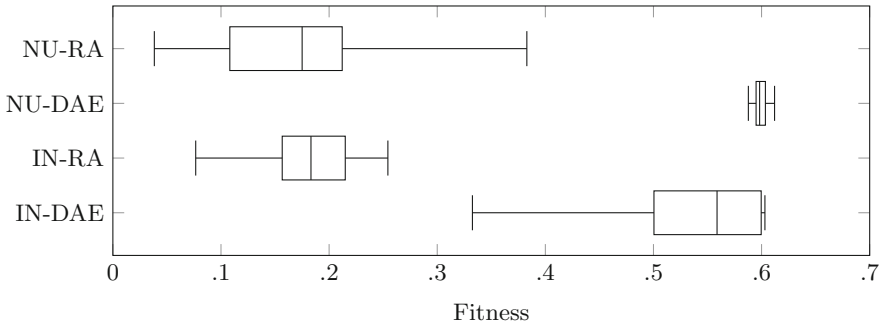

Fig. 6. Comparison of the four contact model variations in a box-and-whisker plot. Approximately 60% fitness were reached with differential-adhesion-energy-dependent (DAE) models. The highest results was accomplished by the model with an additional nutrient-dependent grow on top of the DAE process. Number of simulation runs per model: IN-RA: = 26, NU-DAE = 14, IN-DAE = 26, NU-RA = 37. The x-axis shows only part of the fitness which goes from 0 to 1.

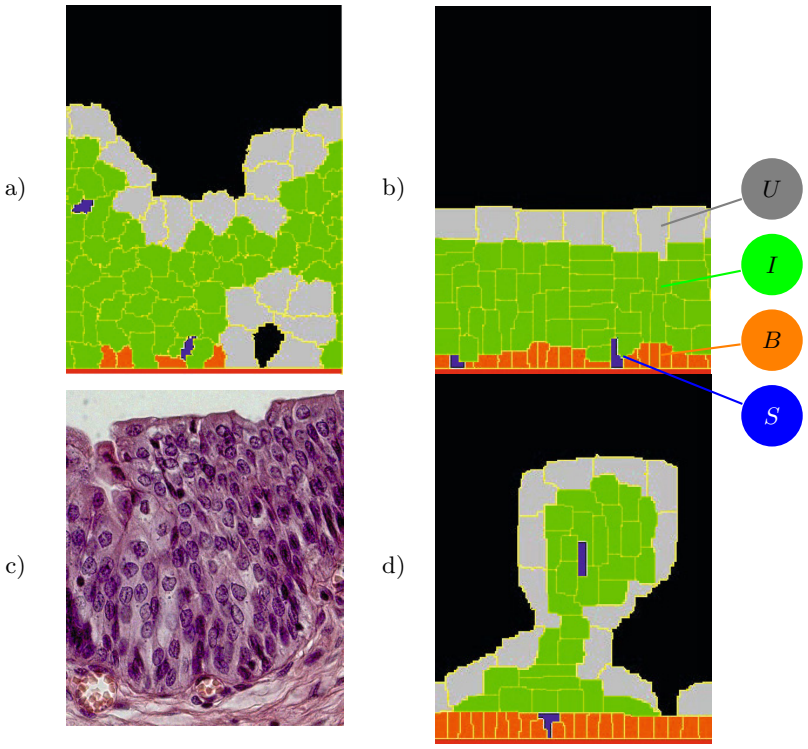

Fig. 7. a) Tissue formation without sort process (IN-RA). b) Simulation in steady state showing a healthy urothelium (NU-DAE). c) Histological image of the urothelium (Hematoxylin and eosin stain). d) Simulated formation of a polyp (IN-DAE).

Figure 7d) shows the deformation of the apical surface of an IN-DAE model. This malformation resembles a polyp, which is often encountered in the bladder lumen. These polyps are mostly benign, but they do have the potential of penetrating through the deeper tissues and of compromising the bladder and other organ function. These polyp-like structures are the reason for the bad fitness at a level as low as 33% observed in the IN-DAE models (cf. 6).

4 Discussion

The contact model was inspired by discoveries from Ho *et al.* [7] and Yamany *et al.* [8]. The suggested cell lineage of Ho *et al.* is especially similar to our approach. Both approaches allow progenitor cells to be responsible for the generation of intermediate cells that can further differentiate into superficial cells. This is supported by the data presented showing that the NU-DAE model reached about 60% of the fitness function.

It remains to be known how the contact model differs from or shares ideas with known hypotheses on cell proliferation for other tissues such as small intestine [22] or epidermis [23]. As the results show in figure 6, it was remarkable that the models IN-DAE and NU-DAE reached the highest fitness values, proving that differential adhesion energies are essential to maintain an organized and stable tissue throughout time. The difference between IN-DAE and NU-DAE can be noticed in the range of the fitness values. While in IN-DAE models the nutrient resources are never scarce the NU-DAE model has limited nutrients, permeating only to about half the ideal urothelium thickness, keeping the randomly escaping stem cells in check by starving them or eventually driving them back to the basal membrane. This rearrangement of the stem cell was due to the fact that without nutrients to divide there was no mitotic pressure to push the stem cell upwards leaving the stem cell enough time to reorganize accordingly to their differential adhesion values.

Urothelial carcinoma of the bladder can be divided into high-grade and low-grade tumors. High-grade tumors are very aggressive and have a risk of muscle invasion, they can present polypoid but can also present as a superficial carcinoma-in-situ. On the other hand low-grade tumors are usually papillary, confined to the mucosa and do not invade the detrusor muscle [14]. They may present as papillary tumors. The formation of polyps in the IN-DAE model demonstrate the potential benefit of this model for further biological questions in bladder cancer [24].

The cellular automaton approach from Kashdan and colleagues [9] showed that carcinogens are important for the development of bladder cancer. In contrast, this work shows the key components for maintaining a healthy urothelium *in silico*. It is also possible to integrate carcinogens fields in our models, as was done with the diffusion field of nutrients introduced in this paper.

It should also be mentioned that the contact model, as such, provides a sort mechanism. It prefers basal cells to be created close to the basal membrane and umbrella cells to be created at the surface. This is some sort of negative feedback mechanism for the differentiation process.

The fitness function we introduced allowed an easy evaluation and visualization of individual simulations. An average fitness of about 60% for a simulation run of NU-DAE models indicates that there could be better models. These simulations often have an excellent arrangement fitness of more than 90% but a poor volume fitness with less than 30% (data not shown). On the one hand, we believe that parameter optimization will improve the fitness. On the other hand, the narrow width of the volume fitness function's peak (compare figure 4) may cause a rapid decrease of the fitness when the volume of the cells shifts only a little away from the optimum. Clearly, a further validation of the *in silico* models is required. However, we found that data addressing turn over times and cell cycles are rare in the literature.

5 Conclusion

In this work we were able to successfully simulate the healthy urothelium in steady state with the GGH-method. A urothelium-dependent fitness function was defined, which enables the quantitative evaluation of the simulation's output. Models for the urothelium that use flexible cell shapes and non-lattice-based cell movements were applied for the first time. They showed that a sorting process and a limited proliferation mechanism appears to be essential. Changes in these parameters are possible mechanisms for the development of cancer.

Acknowledgment. We would like to thank Thomas Ihme for his CUDA server.

References

[1] Jemal, A., Bray, F., Center, M.M., Ferlay, J., Ward, E., Forman, D.: Global cancer statistics (March, April 2011)
[2] Wein, A.J., Kavoussi, L.R., Campbell, M.F., Walsh, P.C.: Campbell-Walsh urology, 10th edn. Elsevier Saunders, Philadelphia (2012)
[3] Paulsson, M.: Basement membrane proteins: structure, assembly, and cellular interactions. Critical Reviews in Biochemistry and Molecular Biology 27(1-2), 93–127 (1992)
[4] Liotta, L.A., Tryggvason, K., Garbisa, S., Hart, I., Foltz, C.M., Shafie, S.: Metastatic potential correlates with enzymatic degradation of basement membrane collagen. Nature 284(5751), 67–68 (1980)
[5] Kubota, Y., Kleinman, H.K., Martin, G.R., Lawley, T.J.: Role of laminin and basement membrane in the morphological differentiation of human endothelial cells into capillary-like structures. The Journal of Cell Biology 107(4), 1589–1598 (1988)
[6] Khandelwal, P., Abraham, S.N., Apodaca, G.: Cell biology and physiology of the uroepithelium. Am. J. Physiol. Renal. Physiol. (297), F1477–F1501 (2009)
[7] Ho, P.L., Kurtova, A., Chan, K.S.: Normal and neoplastic urothelial stem cells: Getting to the root of the problem. Nature Reviews Urology 9(10), 583–594 (2012)
[8] Yamany, T., van Batavia, J., Mendelsohn, C.: Formation and regeneration of the urothelium. Curr. Opin. Organ Transplant. 19(3), 323–330 (2014)

[9] Kashdan, E.: Hybrid discrete-continuous model of invasive bladder cancer. Mathematical Bioscience and Engineering 10(3), 729–742 (2013)
[10] Balter, A., Merks, R.M.H., Popławski, N.J., Swat, M., Glazier, J.A.: The glazier-graner-hogeweg model: Extensions, future directions, and opportunities for further study. Single-Cell-Based Models in Biology and Medicine, 151–167 (2007)
[11] Swat, M.H., Thomas, G.L., Belmonte, J.M., Shirinifard, A., Hmeljak, D., Glazier, J.A.: Multi-scale modeling of tissues using compucell3d. Computational Methods in Cell Biology, 325–366 (2012)
[12] Kreft, M.E., Sterle, M., Veranic, P., Jezernik, K.: Urothelial injuries and the early wound healing response: Tight junctions and urothelial cytodifferentiation. Histochemistry and Cell Biology 123(4-5), 529–539 (2005)
[13] Hicks, R.M.: The mammalian urinary bladder: An accommodating organ. Biol. Rev. Camb. Philos. Soc. 50(2), 215–246 (1975)
[14] MD, M.J.D.: Urothelial Tumors (ACS ATLAS OF CLINICAL ONCOLOGY) (American Cancer Society Atlas of Clinical Oncology). pmph usa (2004)
[15] Steinberg, M.: On the mechanisms of tissue reconstruction by dissociated cells. i. population kinetics, differential adhesiveness, and the ab- sence of directed migration. PNAS 48, 1577–1582 (1962)
[16] Glazier, G.: Simulation of the differential adhesion driven rearrangement of biological cells. Phys. Rev. E Stat. Phys. Plasmas Fluids Relat. Interdiscip. Topics 47(3), 2128–2154 (1993)
[17] Gasser, T.: Basiswissen Urologie, 5th edn. Springer, Heidelberg (2011)
[18] Rübben, H. (ed.): Uroonkologie. 6., aufl. 2013 edn. Springer, Berlin (2013)
[19] Hautmann, R., Huland, H.: Urologie: Mit 176 Tabellen, 4th edn. Springer, Heidelberg (2010)
[20] Hallscheidt, P., Haferkamp, A.: Urogenitale bildgebung. Springer, Berlin (2010)
[21] Schultz-Lampel, D., Goepel, M., Haferkamp, A.: Urodynamik, 3rd edn. Springer, Berlin (2012)
[22] Gumbel, M., Werner, O., Zajicek, G., Meinzer, H.P.: Simulation and 3-d visualization of the intestinal crypt. SCS Publications, pp. 310–312 (1998)
[23] Li, X., Upadhyay, A.K., Bullock, A.J., Dicolandrea, T., Xu, J., Binder, R.L., Robinson, M.K., Finlay, D.R., Mills, K.J., Bascom, C.C., Kelling, C.K., Isfort, R.J., Haycock, J.W., MacNeil, S., Smallwood, R.H.: Skin stem cell hypotheses and long term clone survival – explored using agent-based modelling. Sci. Rep. 3, 1904 (2013)
[24] Shah, J.B., McConkey, D.J., Dinney, C.P.N.: New strategies in muscle-invasive bladder cancer: On the road to personalized medicine. Clin. Cancer Res. 17(9), 2608–2612 (2011)